RINOPOLYCRETE - TOWARDS A CEMENT-FREE AND FULLY RECYCLED CONCRETE

PROJECTO FCT

PTDC/ECI-COM/29196/2017

Recycled inorganic polymer concrete - Towards a cement-free and fully recycled concrete

(RInoPolyCrete)

Task 3 - Report 3

Alkali activation of electric arc furnace slag: Optimum concentration of the alkali activator and mechanical performance of mortars

April 2021

Financiamento FCT/POCI

Governo da República Portuguesa

União Europeia FEDER

FCT Fundação para a Ciência e a Tecnologia

MINISTÉRIO DA CIÊNCIA E DO ENSINO SUPERIOR Portugal

TÉCNICO LISBOA

CERIS Civil Engineering Research and Innovation for Sustainability

TABLE OF CONTENTS

LIST OF ACRONYMS

EAFS	Electric arc furnace slag
AAEAFS	Alkali activated electric arc furnace slag
AAM	Alkali activated material
NaOH	Sodium hydroxide
SiO_2	Silicon oxide
Na_2O	Sodium oxide
Na_2SiO_3	Sodium silicate
CO_2	Carbon dioxide
WRA	Water reducing admixture
CS	Compressive strength
FS	Flexural strength
FA	Fly ash

LIST OF FIGURES

LIST OF TABLES

1 Introduction

In this study, electric arc furnace slag (EAFS) is examined as potential full replacement of cement in the production of alkali-activated mortars. The EAFS used in this study, which is a by-product of steel manufacturing, was provided by HARSCO from the beneficiated output at Siderurgia Nacional, Portugal. The experimental work described in this report concerns the use of alkali-activated electric arc furnace slag (AAEAFS) in mortars, focusing on the optimization of the alkaline activator to achieve maximum mechanical performance. It describes the several stages, starting with EAFS preparation used in the campaign, as well as the other materials typically used in the production of alkali-activated materials (i.e. aggregates and alkaline activators). It presents the mix design of all planned mortars and the testing methodology of fresh and hardened mortars, including slump; shrinkage; flexural strength (FS); compressive strength (CS); and carbonation. Given its extensive particle size distribution, milling of the EAFS was required to achieve a cement-like sized powder before it could be used as a precursor in alkali activation. Different combinations of sodium hydroxide (NaOH) and sodium silicate (Na_2SiO_3) were tried, by varying the Na_2O/binder (4%; 6%; 8%; 10%; 12%) and SiO_2/Na_2O (0; 0.5; 1.0; 1.5; 2.0; 2.5) ratios, to maximize the mechanical performance. The alkaline activators were prepared 24 h prior to the mixing to attain a similar temperature for all mixes. The correlation between the various tested parameters was analysed in order to identify the optimum combination that yields the highest 28-day compressive strength and subsequently quantifying the effect imposed by the accelerated carbonation process on the strength of AAEAFS mortars.

2 Experimental investigation

2.1 Materials and mix proportion

2.1.1 Electric arc furnace slag (EAFS)

EAFS is a by-product of steel manufacturing collected from the Siderurgia Nacional de Portugal, provided by HARSCO. It presents an extensive particle size distribution and requires preparation and grinding in order to be used as binder as shown in Figure 1. This material presents

an apparent density of 3770 kg/m^3. The oxide chemical composition of the raw material, obtained from X-ray fluorescence (XRF), is presented in Table 1. This EAFS contains 28.48% Fe_2O_3, 28.18% CaO, 17.66% SiO_2, and 10.13% Al_2O_3. The high amount of iron in EAFS could induce magnetic properties on AAEAFS concrete [1]. Hafez et al. [2] stated that the amount of aluminosilicate is sufficient to allow this material to contribute as a binder. However, dimensional instability of concrete may occur due to the presence of CaO [3].

Table 1: Chemical composition of EAFS (%)

Fe_2O_3	CaO	SiO_2	Al_2O_3	MgO	MnO_2	Cr_2O_3	TiO_2	P_2O_5	SO_3	Na_2O	BaO	K_2O	V_2O_5	CuO	ZnO
28.48	28.18	17.66	10.13	5.66	5.44	2.38	0.65	0.42	0.33	0.19	0.17	0.03	0.11	0.02	0.02

Figure 1 - Preparation and grinding process of EAFS

2.1.2 Alkaline activator

In this study, the alkaline activator was prepared in terms of a liquid solution. Reactive grade anhydrous sodium hydroxide pellets (NaOH), with 98% purity and a density of 2.13 g/ml, then dissolved in a solvent: tap water complying with Directive 98/83/CE [4]. A commercial solution of sodium metasilicate was used, containing a sodium oxide (Na_2O) content of 8 ± 0.6%, silicon oxide (SiO_2) of 26.4 ± 1.5% and water content of 65.6 ± 2%. It presented a relative density of 1.355 g/ml.

2.1.3 Fine aggregate

Two types of fine siliceous aggregates were used for mortar production. The first type was coarse

sand 0/4, and the second type was fine sand 0/1. The bulk density, water absorption, humidity, and size have been evaluated prior to the use of these fine aggregates as shown in Table 2.

Table 2 - Characterization of the aggregates used in the mortar mixes

Aggregates	Nominal size	Oven-dried density	Water absorption	Mass ratio
	mm	kg/m^3	%	%
Fine sand	0/1	2637	0.4	30
Coarse sand	0/4	2617	0.5	70

2.1.4 Water reducing admixture

The water reducing admixture (WRA) used in this campaign is SikaPlast-717, consisting of a synthetic organic water-based naphthalene dispersant, having density of 1.21 ± 0.03 kg/dm^3 and a pH of 10 ± 1.

2.2 Mortar mix design

The experimental campaign focused on the optimization of the alkaline activator, which was carried out based on the mortar's mechanical performance. The variables are presented in Table 3. To achieve the optimum activator for EAFS, the Na_2O/precursor mass ratio varies between 0.04 and 0.12. The SiO_2/Na_2O ratio varies between 0 and 2.5. The same curing temperature and time of 80 °C and 24 hours, respectively, were applied to all mortars.

Table 3 - Operationalization of the variables

Factor	Unit	Variation
Na_2O/precursor	%	4 6 8 10 12
SiO_2/Na_2O ratio	Dimensionless	0 0.5 1.0 1.5 2.0 2.5
Curing temperature	°C	80
Curing time	Hours	24

The amount of each constituent has been calculated based on some volumetric and mass ratios, using the densities of each of the raw materials. The binder/aggregate volumetric ratio (V_B/V_A) is of 0.33. The mass ratio of SiO_2/Na_2O is 0, 0.5, 1.0, 1.5, 2.0, and 2.5. The mass ratio of water/binder (M_W/M_B) has been fixed and equal to 0.3. The mass WRA/precursor ratio is equal to 1% for all mixes and Na_2O/binder is 4%, 6%, 8%, 10%, and 12%.

2.3 Production method

Mortar production was based on EN 196-1 [5]. The alkaline solution was prepared by dissolving the NaOH pellets in water gradually and then left to cool down for 24 hours. The 40×40×160 mm^3 steel moulds were completely wrapped with thin plastic film to eliminate the use of any releasing agent. The alkaline solution was added first in the mixer along with the WRA and the precursor and then mixed for 3 minutes. After that, the mixer was stopped until the fine aggregates were added and then all the components were mixed for another 2 minutes and 1 additional minute in higher mixing speed was applied. After that, the slump was tested on the slump table as shown in Figure 2 according to EN 1015-3 [6]. Afterwards, the mix was moulded and covered with plastic film and immediately placed in a thermal curing chamber at 80 °C for 24 hours. Finally, the specimens were demoulded, and each specimen was sealed and placed to cure in a dry chamber with a temperature of 23 ± 2 ºC and a relative humidity of 65% until testing day.

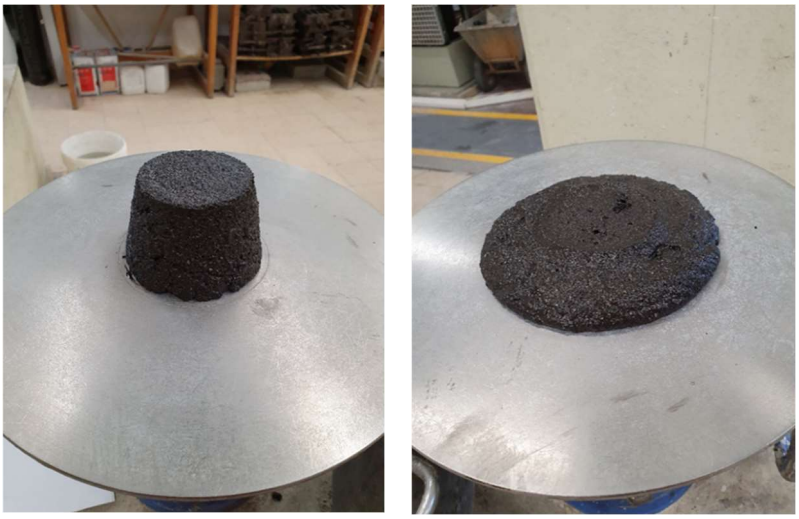

Figure 2 - Slump test

2.4 Curing conditions

Once the mortars were moulded and wrapped with plastic film, they were transported to thermal curing for 24 hours in the treatment oven at a temperature of 80 °C. At the end of this

stage, the mortars were demoulded and placed in their designated curing condition depending on the desired test method, as shown in Table 4.

Table 4 - Curing conditions, test methods and number of specimens of the experimental campaign

Test	Standard	Number of specimens	Curing conditions
Flexural strength Compressive strength	EN 1015-11 [7]	6	Specimens placed sealed in dry chamber until testing age.
Accelerated carbonation	EN 13295 [8]	4	14 days sealed and another 14 days unsealed in the dry chamber; then placed in the carbonation chamber until testing age.
Shrinkage	EN 1015-13 [9]	2	Specimens placed in dry chamber sealed after demoulding until the end of the test.

2.5 Test approaches

The flexural strength test was performed on hardened state mortar prisms of 40×40×160 mm^3, simply supported at both ends and with a load applied at mid-point, as presented in Figure 3. The flexural strength was calculated according to EN 1015-11 [7] as shown in equation 1.

The two halves of the same specimen from the flexural test are after that used and aligned with a 40 × 40 mm^2 compressor. The hydraulic jack starts to compress the specimen until failure as presented in Figure 4. The compressive strength test was done according to EN 1015-11 [7] and calculated by equation 2.

$$fi = 1.5\frac{F_i \; x \; L}{b_i \; x \; d_i^2} \qquad (1)$$

$$c_i = \frac{C_i}{A_i} \qquad (2)$$

Figure 3 - Flexural strength

Figure 4 - Compressive strength

The accelerated carbonation test was performed by placing the mortar specimens, being cured in the dry chamber sealed for 14 days and unsealed for another 14 days in the carbonation chamber, which contained 5 ± 0.1% of CO_2 at room temperature (23 ± 3 °C) and with a relative humidity of 60 ± 5%. This process allowed identifying the resistance against carbonation. The depth of carbonation has been measured by applying phenolphthalein indicator of the split face of the prism after testing for flexural strength of the carbonated specimen according to LNEC E-391 [10]. Natural carbonation is another approach for testing CO_2 penetration by placing the specimens in the dry chamber or in a room where the specimens are exposed to CO_2. However, this process requires more time and is slower than the accelerated carbonation to have the specimens completely carbonated. This study also included shrinkage of the hardened state mortars,

measured according to EN 1015-13 [9]. The routine of measuring the shrinkage of the AAEAFS specimens were as follows:

- Daily for 7 days from mixing day (1 week);
- Every 2 days until the 14th day from mixing day (1 week);
- Every 3 days until the 35th day from mixing day (3 weeks);
- Weekly until the 91st day from mixing day (8 weeks).

3 Results and discussions

21 different mixes were produced to investigate the optimum concentration of the alkali activator in EAFS mortars. All the results are detailed in Table 6, Figure 6 and Figure 7.

3.1 Workability

The mortar's workability was evaluated by their slump according to the EN 1015-3 [6] standard with the values shown in Table 5. The superplasticizer was used and adjusted accordingly depending on the Na_2O/binder and SiO_2/Na_2O ratios. As the Na_2O/binder ratio increased, workability decreased. This was due to the higher viscosity of the alkaline solution after the addition of a solid solute. It was also expected that mixes would lose workability after a short period of time for higher SiO_2/Na_2O ratios due to the well-known flash setting; Ca^{2+} ions from the EAFS quickly react with the silicate ions of the solution, leading to the precipitation of an initial C-S-H, responsible for the setting [11]. Therefore, it can be stated that there is a correlation between workability and Na_2O/binder and SiO_2/Na_2O ratios. The target slump had been initially set at 140 ± 20 mm. However, mixes MS13, MS14 and MS15 presented a lower slump due to the increase in viscosity of the alkaline activator. Therefore, the superplasticizer content increased for mixes with silicate modulus equal to or more than 1.5.

Table 5 - Slump test results (* mixes to repeat)

Mix	W/B ratio	SiO_2/Na_2O	WRA	Slump (mm)
MS1	0.4	0	0.0%	194
MS2				206
MS3				199
MS6	0.3	0.5	0.5%	*
MS7				*
MS8				137
MS9				*
MS10				*
MS11		1.0		152
MS12				148
MS13				117
MS14				117
MS15				109
MS16		1.5	1.0%	147
MS17				130
MS18				134
MS19		2.0		140
MS20				144
MS21		2.5		136

3.2 Compressive strength

The average compressive and flexural strength of AAEAFS is shown in Table 6. Figure 6 presents how significantly compressive strength is influenced by different parameters. The alkali activator is the most important factor controlling compressive strength. Different studies on alkali-activated materials used at least one of the alkaline activators stated in this study. Turker et al. [12], Ozturk et al. [13], and Peys et al.[14] used both sodium hydroxide and sodium silicate to obtain compressive strength values of 40.7 MPa, 22.0 MPa, and 16.0 MPa, respectively, while Abdollahnejad et al. [15] used only sodium hydroxide and achieved 27.0 MPa. However, the maximum compressive strength in this study for uncarbonated specimens was 9.61 MPa in mixes

with 4% and 2.5 for Na_2O/binder and SiO_2/Na_2O ratios, respectively. Furthermore, mixes MS4 and MS5 had values close to zero. This could be due to the excess amount of sodium hydroxide and the lack of sodium silicate. Increasing the amount of Na_2O until a certain percentage increases the strength, after which the performance starts to deteriorate. Nevertheless, excess amount of OH^-, due to the $Ca(OH)_2$ across the particles of EAFS, reduces the interaction of Ca^{2+} ions from the surface of EAFS [16]. Therefore, it can be stated that the low strength is because of the inadequate amount of C-S-H gels produced by the reaction of Ca^{2+} with Si^{4+}.

Sodium hydroxide and sodium silicate have a significant influence on the mechanical properties of AAEAFS. Si^{4+} and Al^{3+} ions within the EAFS dissolve much more with high concentration of OH^- [17]. Song et al. [18] observed that increasing the concentration of the alkali activator increases the reaction rate as a result of high alkali medium.

Wang et al. [19] stated that sodium hydroxide and sodium silicate are directly proportional to compressive strength only to a certain level from 3-5% by weight of the mix. The authors also stated that, if the amount of sodium concentration increased, it would cause efflorescence, as shown in Figure 5. This is due to the migration of Na^+ ions to the surface of the specimens, leading to the precipitation of sodium carbonate.

Figure 5 - Efflorescence caused by Na_2CO_3

Another parameter affecting the compressive strength for all the mixes was time. The specimens in this study experienced 7-days, 28-days, and 91-days of curing time in a dry chamber at 23 ± 2 ºC. Since all specimens were sealed, there were no exchanges of humidity with the surrounding environment. The maximum compressive strength of the same alkali activator combination stated earlier in this section was obtained at 91-days of curing. However, the compressive strength has increased significantly by forcing CO_2 into the specimen, as detailed in section 3.4.

3.3 Flexural strength

Table 6 and Figure 7 present the results observed for the flexural strength of AAEAFS mortars in which the maximum average strength achieved was 7.85 MPa for the same optimum mix as the one observed for compressive strength. However, the surface of the specimens presented some microcracks. Ya-Min et al. [20] stated that this may be due to the heat curing process and the expedited nature of the reactions at relatively high temperature levels, which may have induced a significant amount of microcracks thereby resulting in reduced strength. Although a higher SiO_2/Na_2O ratio is a good indicator of an improved performance [17, 21-23], it is possible that the low performance in the case of the EAFS is due to the low amount of amorphous phases present in the precursor, which did not react with the alkaline activator. Furthermore, even though one would expect to have improved performance from the interaction of Ca from the EAFS with the SiO_2 from the activator to produce C-S-H gels, it is possible that the Ca-bearing mineralogical phases were stable at high pH levels, thereby minimizing the dissolution of Ca^{2+} ions to the solution.

Silicate modulus and sodium concentration had an obvious effect on the mechanical performance. Contrary to expected, the flexural strength of mixes with lower performance is often not correlated with the compressive strength (Figure 8). Figure 9 suggests otherwise for carbonated specimens with enhanced performance, in which exponential relationships were observed between the flexural and compressive strength. However, both flexural strength and compressive strength increased by increasing curing time and curing condition. While the latter typically presented peak performance for specific Na_2O/binder ratios, flexural strength was directly proportional to that ratio.

Table 6 - Compressive (CS) and flexural (FS) strength results from uncarbonated and carbonated specimens at different testing ages (n/a - specimens with insufficient stability; * mixes to be repeated due to inconsistent values)

Mix	Na_2O/binder (%)	SiO_2/Na_2O	7-days curing		28-days curing		91-days curing		7-days CO_2 cured		28-days CO_2 cured	
			FS (MPa)	CS (MPa)	FS (MPa)	CS (MPa)	FS (MPa)	CS (MPa)	FS (MPa)	CS (MPa)	FS (MPa)	CS (MPa)
MS1	4	0.0	0.32	1.12	0.77	1.63	1.13	2.22	2.16	5.74	4.29	9.80
MS2	6	0.0	0.56	1.32	0.96	1.99	1.48	3.29	2.63	5.32	3.73	10.97
MS3	8	0.0	0.58	1.28	0.87	1.69	1.36	2.91	2.51	4.53	3.54	7.71
MS4	10	0.0	n/a	n/a	n/a	n/a	n/a	n/a	n/a	n/a	n/a	n/a
MS5	12	0.0	n/a	n/a	n/a	n/a	n/a	n/a	n/a	n/a	n/a	n/a
MS6	4	0.5	*	*	*	*	*	*	*	*	*	*
MS7	6	0.5	*	*	*	*	*	*	*	*	*	*
MS8	8	0.5	1.33	3.21	1.09	3.60	1.64	5.22	3.98	20.19	3.98	22.30
MS9	10	0.5	*	*	*	*	*	*	*	*	*	*
MS10	12	0.5	*	*	*	*	*	*	*	*	*	*
MS11	4	1.0	1.01	3.70	1.39	4.59	0.95	5.26	1.98	11.63	2.28	12.18
MS12	6	1.0	1.27	4.30	1.46	5.67	1.39	7.46	2.75	18.61	2.96	19.55
MS13	8	1.0	1.41	3.62	1.50	4.49	1.48	6.60	4.24	22.11	5.87	28.21
MS14	10	1.0	1.20	3.25	1.41	3.72	1.63	5.16	5.70	22.67	6.54	28.51
MS15	12	1.0	1.66	3.70	1.57	3.89	2.45	5.58	5.27	14.89	7.85	31.11
MS16	4	1.5	0.89	4.95	0.80	5.18	0.86	5.74	2.00	13.45	2.70	13.74
MS17	6	1.5	1.33	4.29	0.96	4.17	1.25	5.81	3.75	22.31	5.51	23.54
MS18	8	1.5	2.06	5.45	1.62	5.99	1.77	7.85	5.84	28.98	7.73	30.17
MS19	4	2.0	0.91	6.16	1.01	7.40	0.62	9.08	1.86	19.57	4.64	21.50
MS20	6	2.0	1.10	6.75	1.27	8.15	0.66	9.03	1.79	20.35	4.52	21.38
MS21	4	2.5	1.22	8.63	1.34	9.07	0.59	9.61	1.41	14.36	3.96	17.40

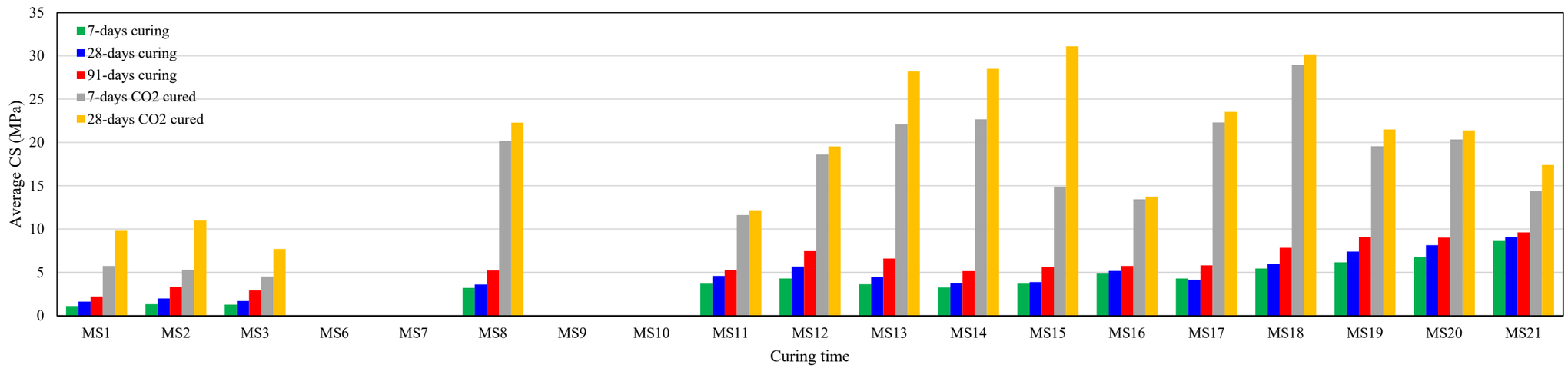

Figure 6 - Average compressive strength (CS)

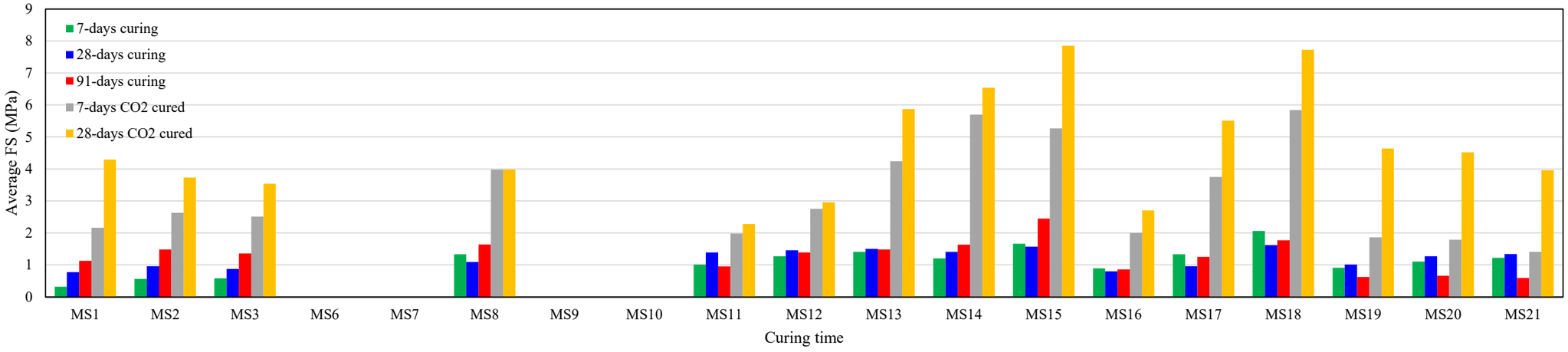

Figure 7 - Average flexural strength (FS)

3.4 Carbonation

The average compressive and flexural strengths of specimens subjected to accelerated carbonation are shown in Table 6, Figure 8 and Figure 9. A noticeable improvement of the mechanical performance of AAEAFS mortars was observed. The additional 28 days of accelerated carbonation led to a near 800% increase in compressive strength from 3.9 MPa in uncarbonated mixes to 31 MPa. This maximum mechanical performance was obtained in mixes with 12% and 1.0 for Na_2O/binder and SiO_2/Na_2O ratios, respectively, thus showing a shift in the optimal alkaline activator contents. It is likely that Ca^{2+} ions were released from the EAFS' Ca-bearing phases and reacted with OH^- ions from the alkali activator thereby producing $Ca(OH)_2$. This compound later reacted with the CO_2 forced into the microstructure, resulting in the precipitation in $CaCO_3$ polymorphs, which significantly densified the microstructure and thus increased strength [13, 18].

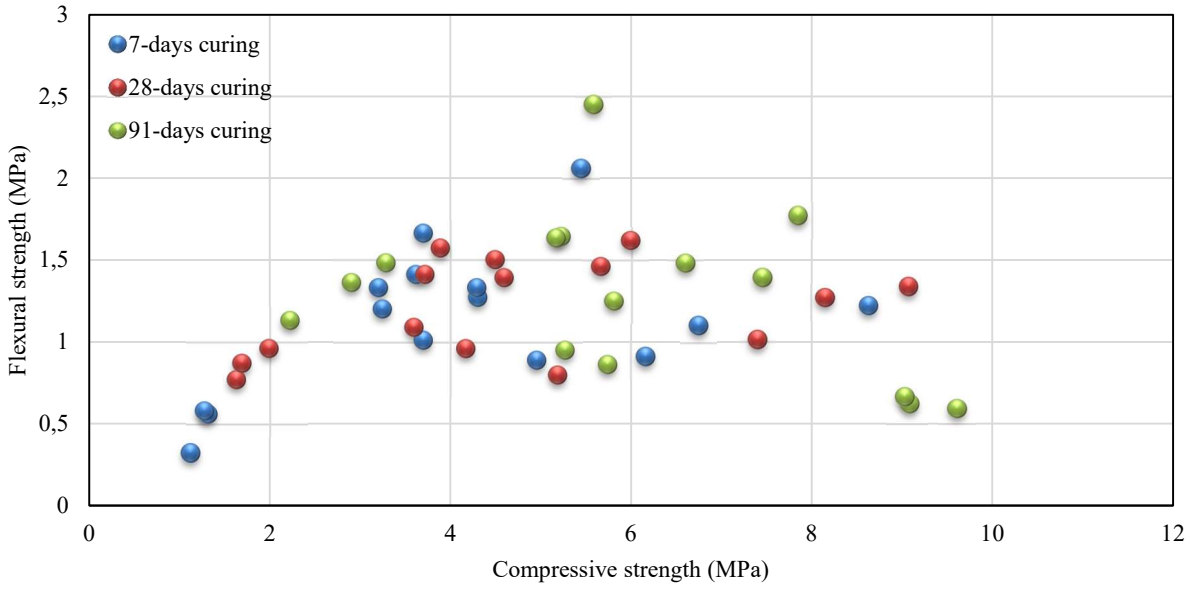

Figure 8 - Flexural vs. compressive strength of uncarbonated specimens

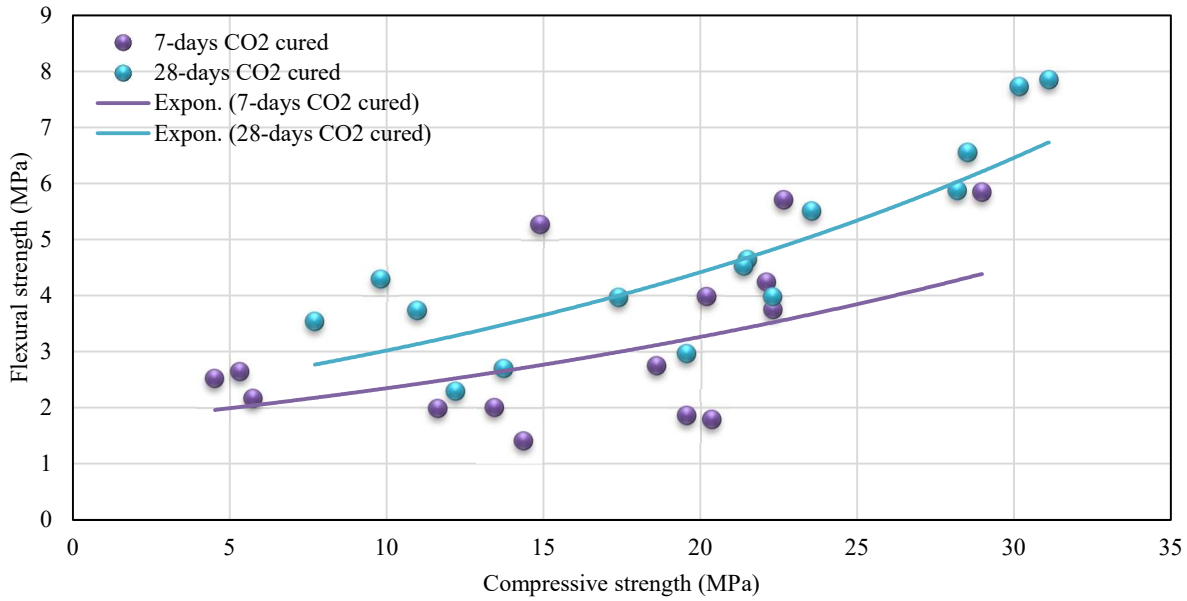

Figure 9 - Flexural vs. compressive strength of carbonated specimens

3.5 Shrinkage

In Figure 10, the change in length (i.e. shrinkage) of sealed specimens with little to no exchange of humidity with the surrounding environment were tested for 91 days. Most specimens presented considerable shrinkage with one of them being close to 3500 µm/m, which is three times higher that typically observed for standard cement mortars. The water may have been mostly used in the alkali activation reaction, leading to a considerable autogenous shrinkage. No correlation with the alkali solution composition was observed. All specimens presented at least 45% of their total 91-day shrinkage in the first 28 days, except for mix MS8. This one slightly expanded, with minor fluctuations, for the first 28 days and started to shrink later on to settle at 198.4 µm/m after 91 days. This behaviour also occurred in fly ash (FA) mortars studied by Atiş et al. [24]. The authors hypothesized that the expansion of mortars containing FA could be from the MgO and the high content of SO_3, which can result in long-term instability due to the formation of expansive calcium sulphate phases [24]. Atiş et al. [24] also stated that materials having expansion properties could be implemented as 'shrinkage-reducing agents' by trial amounts to compensate the shrinkage of cement elements [24].

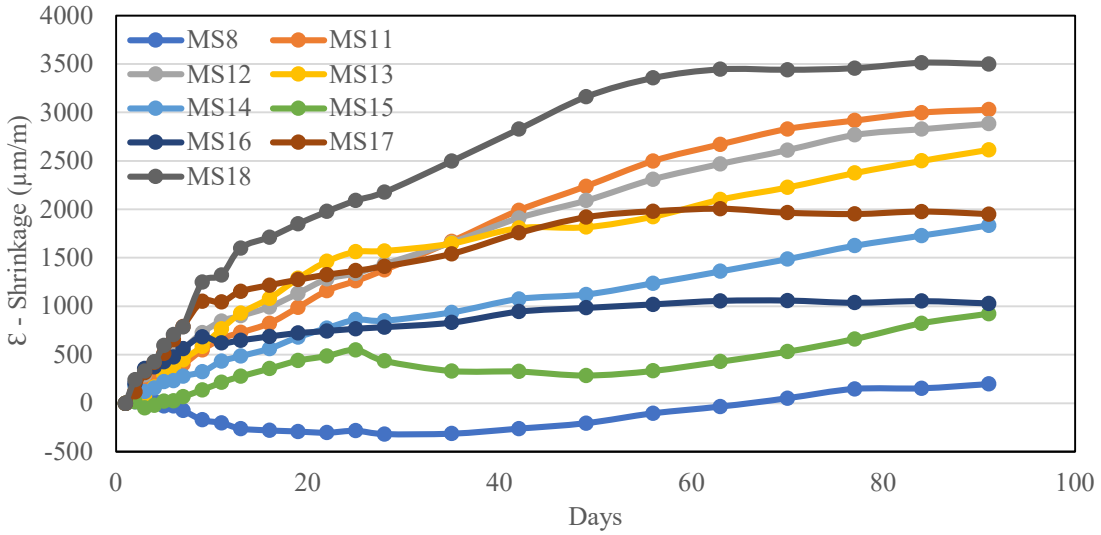

Figure 10 - Shrinkage

4 Conclusions

In this study, electric arc furnace slag (EAFS) was examined as potential full replacement of cement in the production of alkali-activated mortars. The results obtained in this campaign allowed concluding that EAFS as the sole precursor will result in mixes with low performance. This is most likely due to the lower amount of amorphous phases in comparison with other commonly aluminosilicate pozzolans. Regarding the alkali activator's optimal contents, if was found that the SiO_2/Na_2O ratio and compressive strength are generally directly proportional. In fact, the maximum recorded performance of specimens occurred for mixes with 4% and 2.5 for Na_2O/binder and SiO_2/Na_2O ratios, respectively. Another parameter affecting the compressive strength is time, thereby showing continued reaction after the 24 h thermal curing stage. The specimens in this study experienced 7 days, 28 days, and 91 days of curing time in a dry chamber at 23 ± 2 ºC and a relative humidity of 65%. The maximum recorded compressive strength was obtained at 91 days of curing (4% Na_2O/binder ratio and 2.5 SiO_2/Na_2O ratio).

However, in spite of the shortcomings of EAFS as sole precursor, the mechanical performance increased significantly after subjecting the specimens to an accelerated carbonation stage. After subjecting 28 days to a CO_2-enriched environment, the AAEAFS showed an average compressive strength increase of ~500%, with one case reaching 800% (i.e. from an initial 3.9 MPa in

uncarbonated mixes to 31 MPa). The maximum performance was observed in mixes with 12% and 1.0 for Na_2O/binder and SiO_2/Na_2O ratios, respectively, thus showing a shift in the optimal alkaline activator contents.

The sealed shrinkage test showed considerable dimensional variability over time. Great autogenous shrinkage may have occurred due to the continuous alkali activation reaction. Nevertheless, this phenomenon is still widely unknown and must be further researched.

The complete replacement of cement with alkali-activated aluminosilicate wastes may translate into significant reductions in cost and minimal environmental impacts especially with the incorporation of a forced carbonation curing stage using industrial CO_2-rich flue gases.

Acknowledgments

The authors acknowledge the support of the CERIS Research Institute, IST, University of Lisbon and FCT- Foundation for Science and Technology, through the research project PTDC/ECI-CON/29196/2017 “Recycled Inorganic Polymer Concrete: Towards a fully recycled and cement-free concrete” (RInoPolyCrete). The authors would also like to acknowledge the support of Valorsul, EDP and SIKA for part of the materials provided for this experimental campaign.

References

[1] M. Ozturk, O. Akgol, U.K. Sevim, M. Karaaslan, M. Demirci, E. Unal, Experimental work on mechanical, electromagnetic and microwave shielding effectiveness properties of mortar containing electric arc furnace slag, Constr. Build. Mater. 165 (2018) 58-63.

[2] D.K. Hisham Hafez, Rawaz Kurda, Rui Vasco Silva, Jorge de Brito, Assessing the sustainability potential of alkali-activated concrete from electric arc furnace slag using the ECO2 framework, Constr. Build. Mater. Volume 281 (2021).

[3] I. Arribas, A. Santamaria, E. Ruiz, V. Ortega-Lopez, J.M. Manso, Electric arc furnace slag and its use in hydraulic concrete, Constr. Build. Mater. 90 (2015) 68-79.

[4] U. Europeia, Diretiva 98/83/CE do Conselho, de 3 de novembro de 1998, relativa à qualidade da água destinada ao consumo humano, Jornal Oficial das Comunidades Europeias. L 330 (1998) 32-54.

[5] EN-196-1, Methods of testing cement - Part 1: Determination of strength, Comité Européen de Normalisation (CEN), Brussels, Belgium, 2005, p. 36.

[6] EN-1015-3, Methods of test for mortar for masonry - Part 3: Determination of consistence of fresh mortar (by flow table), Comité Européen de Normalisation (CEN), Brussels, Belgium, 1999, p. 10.

[7] EN-1015-11, Methods of test for mortar for masonry - Part 11: Determination of flexural and compressive strength of hardened mortar, Comité Européen de Normalisation (CEN), Brussels, Belgium, 1999, p. 12.

[8] EN-13295, Products and systems for the protection and repair of concrete structures.Test methods. Determination of resistance to carbonation, Comité Européen de Normalisation (CEN), Brussels, Belgium, 2004, p. 18.

[9] EN-1015-13, Methods of test for mortar for masonry - Part 13: Determination of dimensional stability of hardened mortars, Comité Européen de Normalisation (CEN), Brussels, Belgium, 1993, p. 20.

[10] LNEC-E391, Concrete: determination of carbonation resistance (in Portuguese), National Laboratory in Civil Engineering (LNEC - Laboratório Nacional de Engenharia Civil) Lisbon, Portugal, 1993, p. 2.

[11] A. Fernández-Jiménez, F. Puertas, Setting of alkali-activated slag cement. Influence of activator nature, Advances in Cement Research 13(3) (2001) 115-121.

[12] H.T. Türker, M. Balçikanli, İ.H. Durmuş, E. Özbay, M. Erdemir, Microstructural alteration of alkali activated slag mortars depend on exposed high temperature level, Constr. Build. Mater. 104 (2016) 169-180.

[13] M. Ozturk, M.B. Bankir, O.S. Bolukbasi, U.K. Sevim, Alkali activation of electric arc furnace slag: Mechanical properties and micro analyzes, J. Build. Eng. 21 (2019) 97-105.

[14] A. Peys, L. Arnout, B. Blanpain, H. Rahier, K. Van Acker, Y. Pontikes, Mix-design parameters and real-life considerations in the pursuit of lower environmental impact inorganic polymers, Waste Biomass Valori. 9(6) (2018) 879-889.

[15] Z. Abdollahnejad, C.M. Jesus, F. Pacheco-Torgal, J. Aguiar, One-part geopolymers versus Ordinary Portland Cement (OPC) mortars: durability assessment, (2013).

[16] S.A. Bernal, J.L. Provis, V. Rose, R. Mejía de Gutierrez, Evolution of binder structure in sodium silicate-activated slag-metakaolin blends, Cem. Concr. Compos. 33(1) (2011) 46-54.

[17] C.R. Shearer, J.L. Provis, S.A. Bernal, K.E. Kurtis, Alkali-activation potential of biomass-coal co-fired fly ash, Cem. Concr. Compos. 73 (2016) 62-74.

[18] S. Song, H.M. Jennings, Pore solution chemistry of alkali-activated ground granulated blast-furnace slag, Cem. Concr. Res. 29(2) (1999) 159-170.

[19] S.-D. Wang, K.L. Scrivener, P. Pratt, Factors affecting the strength of alkali-activated slag, Cem. Concr. Res. 24(6) (1994) 1033-1043.

[20] Y.-m. Gu, Y.-h. Fang, D. You, Y.-f. Gong, C.-h. Zhu, Properties and microstructure of alkali-activated slag cement cured at below-and about-normal temperature, Constr. Build. Mater. 79 (2015) 1-8.

[21] S. Caijun, L. Yinyu, Investigation on some factors affecting the characteristics of alkali-phosphorus slag cement, Cem. Concr. Res. 19(4) (1989) 527-533.

[22] M. Criado, A. Fernández-Jiménez, A. De La Torre, M. Aranda, A. Palomo, An XRD study of the effect of the SiO2/Na2O ratio on the alkali activation of fly ash, Cem. Concr. Res. 37(5) (2007) 671-679.

[23] M.N. Qureshi, S. Ghosh, Effect of silicate content on the properties of alkali-activated blast furnace slag paste, Arabian Journal for Science and Engineering 39(8) (2014) 5905-5916.

[24] C.D. Atiş, A. Kilic, U.K. Sevim, Strength and shrinkage properties of mortar containing a nonstandard high-calcium fly ash, Cem. Concr. Res. 34(1) (2004) 99-102.

Lisboa, April 29, 2021

Authors

Dany Azad Kareem Kassim	Rui Vasco Silva
PhD Student	Post-Doc Researcher

Jorge de Brito

Full Professor